# An Efficient Shell Element Based Approach to Modeling the Impact Response of Fabrics

Ali Shahkarami, Reza Vaziri
*Composites Group, Departments of Civil Engineering and Materials Engineering*
*The University of British Columbia, Vancouver, BC, Canada, V6T 1Z4*

## Abstract

*An efficient shell element based computational model is developed to capture the mechanical response of fabrics. The approach considers a single yarn crossover as the basic building block (unit-cell) of the fabric panel and uses a specially formulated shell element within LS-DYNA to capture the essential features of the membrane response of this unit-cell accounting for both geometrical and material characteristics of the yarns. The shell element so developed is used to simulate the impact response of single and multi-ply packs of Kevlar® 129 fabric. The predictions are successfully compared with the measurements obtained from instrumented ballistic impact experiments.*

## Introduction

Dynamic analysis of fabric structures under impact has continued to be a challenging task due to the complex behavior of woven systems. Over the years, numerous modeling techniques have been developed by scientists to capture the complex behavior of fabrics which has contributed to the general knowledge on the dynamic response of these structures in ballistic events. Despite all such efforts, however, there is still a need for a realistic, yet efficient modeling approach to predict the behavior of multi-layer fabrics subjected to ballistic impact.

The numerical approaches developed to capture the ballistic response of fabrics can be divided into two main categories: discrete models and continuum models. Discrete models are based on the representation of a fabric layer as an assembly of discrete elements. These models use one-dimensional string elements to model the warp and weft yarns, pin-jointed to each other at their crossover points in an initially orthogonal fashion. Roylance and Wang [1] proposed one of the earliest models of this type, adopted and modified later by other scientists to investigate the ballistic performance of various fabric targets (e.g., Shim et al. [2], Lim et al. [3], Cepuš et al. [4], Shahkarami et al. [5], Johnson et al. [6], and Billon [7]). The discrete pin-jointed models are very simple in principle and computationally efficient; however, they lack the sophistication needed to realistically represent many geometrical and mechanical aspects of fabrics, such as the interaction between the crossing yarns. Continuum models of fabrics, on the other hand, take advantage of a higher level of complexity to incorporate many of the fabric's characteristic properties overlooked by the discrete models. Highly detailed three-dimensional models of woven fabrics consider the geometry of the fabric through continuum representation of individual yarns in the weave and explicitly capture their interaction under various loading scenarios. Examples of such models can be found in the works of Shockey et al. [8], Tanov and Brueggert [9] and Duan et al. [10]. The 3D continuum models are perhaps the most elaborate computational techniques to date, however, they are computationally intensive even for analysing small sizes of a single ply of fabric, let alone industrial size fabric armor with thicknesses of practical relevance (i.e. 30 to 50 ply packs). Shell-based continuum models smear the interaction of yarns in a woven fabric into a single representative element and are extensively used in the analysis of fabrics and fabric composites. Kawabata [11] presented one of the earliest analytical models to capture the biaxial behavior of a symmetrically loaded yarn cross-over. The authors [12,13] presented a study where an analytical model developed to capture the

interaction of the crossing yarns of a plain weave fabric unit-cell was implemented in a shell element constitutive model. Tabiei and Ivanov [14] developed a shell element that represented a crossover with yarns interlacing at a certain braid and crimp angles. In a recent study, King et al. [15] presented the details of a continuum model relating the macroscopic deformations of the fabric to its structural configuration. The model was intended to be used for fabrics under quasi-static in-plane loads.

In this study a crossover-based unit-cell is used as the basic building block of a full layer of fabric. A constitutive model is developed that considers the nonlinear shape of the yarns to capture their interaction under symmetrically applied displacements. An equivalent (smeared) shell element that captures the biaxial membrane response of an individual layer of fabric under different loading conditions is developed. Finally, the shell-based model is used to predict the ballistic performance of single and multi-ply fabric targets for which experimental data is available.

## Representative Shell Element

The numerical approach proposed here is based on capturing the behavior of yarns in a unit-cell and implementing them into a representative shell element. This shell element is developed within the framework of the explicit finite element code LS-DYNA [16], through the definition of the material constitutive relationship as a User Material Model (UMAT). In this study, the in-plane extensional and shear responses of the unit-cell are assumed to be decoupled.

The in-plane extensional response of the fabric unit-cell is captured based on a realistic representation of the yarns' geometry and mechanical behavior and their interaction under various loading scenarios. The shell element representing a single fabric unit-cell (a single yarn crossover in this case) takes advantage of an analytical model to provide the biaxial response of a yarn crossover for a range of symmetrically applied in-plane displacements. This section describes the fundamentals of the UMAT developed for the shell element representing a single yarn crossover.

The User Material Models in LS-DYNA enable the user to define the constitutive relationship for the elements. For this purpose, the UMAT is provided with the stresses from the previous time-step, as well as the current strain increments, and is required to return the updated stress tensor to the code. In the development of the representative shell element for fabric unit-cells, the displacements applied to the warp and weft yarns and the angle between them need to be calculated from the strain increments at every time-step. To achieve this goal, the deformation gradient, $\underline{F}^n$, pertaining to the incremental changes in the displacement field between the two consecutive time steps $n-1$ and $n$ can be assembled from the strain increments as follows:

$$\underline{F}^n = \left(\underline{I} + 2\underline{\Delta\varepsilon}^n\right)^{0.5} \approx \underline{I} + \underline{\Delta\varepsilon}^n = \begin{bmatrix} 1+\Delta\varepsilon_x{}^n & \Delta\varepsilon_{xy}{}^n \\ 0 & 1+\Delta\varepsilon_y{}^n \end{bmatrix} \tag{1}$$

where $\underline{\Delta\varepsilon}^n$ is the tensor of the strain increments with components $\Delta\varepsilon_x{}^n$, $\Delta\varepsilon_y{}^n$ and $\Delta\varepsilon_{xy}{}^n$ in the local coordinate system $xyz$, and $\underline{I}$ is the 2x2 unit matrix. The shell local axes system in LS-DYNA is based on its node numbering, as defined in the User's Manual [16]. In the convention used in this study, the local $x$-axis is defined to be parallel to the shell edge connecting its first two nodes. The $z$-axis is normal to the element mid-plane and the $y$-axis is determined by the cross product

$$y = z \times x \tag{2}$$

The material axes, on the other hand, are assumed to be parallel to the warp and weft yarns. The strain increments resulting from the deformation of the element need to be converted into the unit-cell displacements in the material directions (along warp and weft yarns) to determine the biaxial response of the crossover. In the un-deformed configuration, the material and local axes coincide in the case of uniform rectangular elements. As the element undergoes large displacements and rotations, the angle between the local and the material axes (defined by the warp and the weft) changes. The angle between the material and element local axes of the element is thus updated at each time step in order to determine the displacements applied to the warp and weft yarns.

To track the configuration of the material axes in the local coordinate system during the analysis, two vectors $q_1$ and $q_2$ are considered parallel to the warp and weft (fill) yarns, respectively (see Figure 1). The position of these two vectors is updated at each time step in the local coordinate system using the deformation gradient as follows:

$$q_i^{\,n} = \underline{F}^{\,n} q_i^{\,n-1} \tag{3}$$

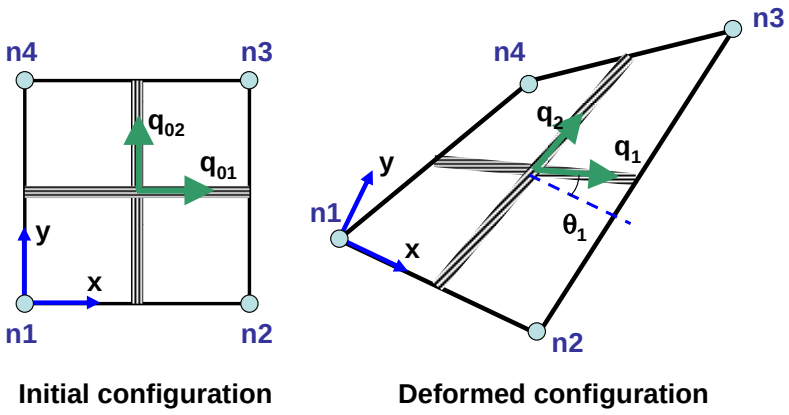


Figure 1: Local element and material axes convention for shell elements in LS-DYNA.

where $q_i^{\,n-1}$ and $q_i^{\,n}$ are the $i$ material vector ($i = 1, 2$ for warp and weft) at time steps $n-1$ and $n$, respectively. The angle between each material vector and the local $x$-axis can be determined as follows:

$$\theta_i^{\,n} = \tan^{-1}\left(\frac{q_{iy}^{\,n}}{q_{ix}^{\,n}}\right) \tag{4}$$

Where

$$q_i^{\,n} = \left[q_{ix}^{\,n} \quad q_{iy}^{\,n}\right]^T \tag{5}$$

The strain increment tensor needs to be transformed into the direction of the two material vectors. The appropriate transformation matrix is calculated for each material vector based on its current angle:

$$\underline{\Theta_i}^{\,n} = \begin{bmatrix} \cos\theta_i^{\,n} & \sin\theta_i^{\,n} \\ -\sin\theta_i^{\,n} & \cos\theta_i^{\,n} \end{bmatrix} \tag{6}$$

The strain increments are subsequently rotated to the material directions using the transformation matrix as follows:

$$\underline{\Delta\varepsilon_i}^{\,n} = \underline{\Theta_i}^{\,n}\,\underline{\Delta\varepsilon}^{\,n}\,\underline{\Theta_i}^{\,nT} \tag{7}$$

The displacements along the yarns can then be calculated using the basics of continuum mechanics. The incremental stretch of a unit vector in the material directions from time step $n-1$ to $n$ can be calculated from the equation below:

$$\lambda_i^{\,n} = \sqrt{1+2\Delta\varepsilon_{i11}^{\,n}} \approx 1+\Delta\varepsilon_{i11}^{\,n} \tag{8}$$

where $\Delta\varepsilon_{i11}^{\,n}$ is the strain component in the yarn axial direction. The total stretch in the material directions is updated at each time step using the incremental stretch values of Equation (8), as shown below:

$$\Lambda_i^{\,n} = \Lambda_i^{\,n-1}\lambda_i^{\,n} \tag{9}$$

The displacement along yarn $i$ at time step $n$ would then be equal to

$$d_i^{\,n} = \Lambda_i^{\,n} w_{0i} \tag{10}$$

where $w_{0i}$ is the projection of the yarn half-length in the fabric plane before the application of the displacements. Knowing the displacements $d_1$ and $d_2$, the analytical model for the in-plane extension of the unit-cell can be used to calculate the tensile forces developed in the warp and weft yarns. The model developed is inspired by Kawabata's linear crossover model [11], with further expansion to accommodate the non-linear geometry of the yarns. The model is based on tracking the location of the yarn centrelines as the two yarns interact under the applied displacements. It is assumed that the yarn profiles of the woven fabric are initially sinusoidal and remain sinusoidal at all times, independent from the details of micro and macroscopic unit-cell displacements. The initial geometry of each yarn centreline is determined by its initial crimp, obtained from the laboratory measurements. The in-plane warp and weft displacements are assumed to be symmetrically applied at the two yarn ends, preventing any sliding between the two crossing yarns. This assumption results in an effectively pin-jointed model, since no relative in-plane yarn displacement occurs at the point of contact between the two yarns. It is assumed that there is no friction between the contacting yarns so that the contact force at any point is perpendicular to the surface of the yarns (Figure 2). For the analysis of the crossover mechanics, only the resultant contact force acting at the centre-point of the crossover is considered. For a unit-cell of initial width $2w_{0i}$ along yarn $i$, the profile of the yarn centreline can be expressed as below, with the origin of coordinates taken to be at the centre of the unit cell:

$$f(x) = z_i = h_{0i}\cos\left(\frac{\pi}{2w_{0i}}x\right) \tag{11}$$

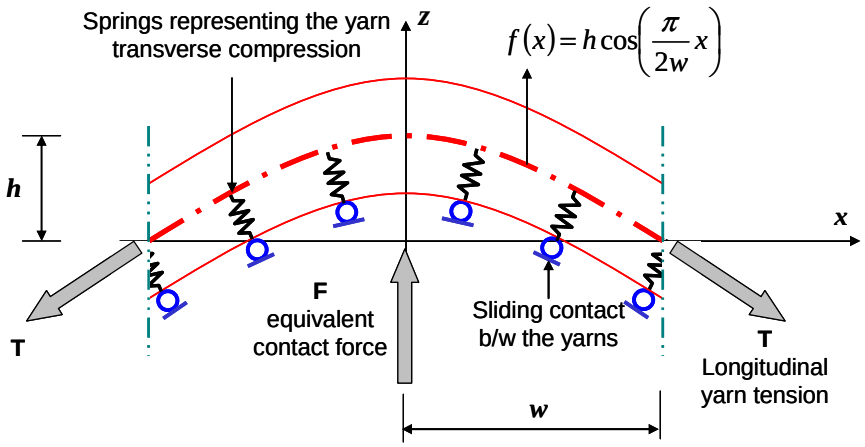


Figure 2: A schematic model of a yarn in the fabric in contact with the crossing yarn, showing the forces acting on it.

where $h_{0_i}$ is the initial height of the yarn centreline at the centre of the unit-cell ($x=0$). The parameter $w_{0_i}$ (in mm) can be calculated from the yarn count, $m$ (in threads/mm), as

$$2w_{0_i}=\frac{1}{m} \tag{12}$$

The value of $h_{0_i}$ can be calculated mathematically from the crimped length of the yarn. Considering the yarn profile function presented in Equation (11), the length, $S_{0_i}$, of the yarn can be calculated from the equation below.

$$S_{0_i}=2\int_0^{w_{0i}}\sqrt{1+\left(\frac{\pi h_{0_i}}{2w_{0_i}}\right)^2\sin^2\left(\frac{\pi}{2w_{0_i}}x\right)}dx \tag{13}$$

The initial length of the yarn can also be determined from yarn crimp, $cr_i$:

$$S_{0_i}=2w_{0_i}(1+cr_i) \tag{14}$$

From Equations (13) and (14), the nonlinear equation needed to calculate the value of $h_{0_i}$ is obtained:

$$w_{0_i}(1+cr_i)=\int_0^{w_{0i}}\sqrt{1+\left(\frac{\pi h_{0_i}}{2w_{0_i}}\right)^2\sin^2\left(\frac{\pi}{2w_{0_i}}x\right)}dx \tag{15}$$

Figure 3 shows a cross-over of two interlacing yarns, with both yarn centrelines shown on the same plane for illustration purposes. The geometry of the yarns after the application of symmetric displacements $d_1$ and $d_2$ can be expressed in terms of their new heights $h_1$ and $h_2$. The goal is to determine the values of the two unknowns, $h_1$ and $h_2$ for a given set of displacements $d_1$ and $d_2$.

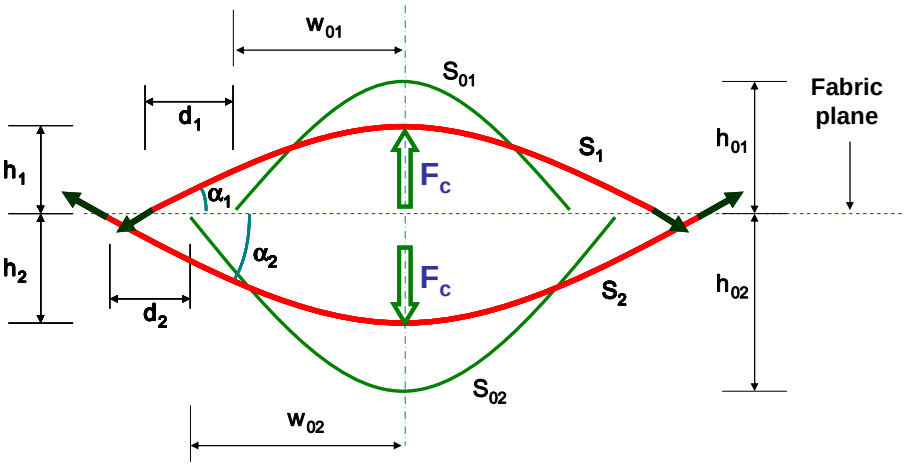


Figure 3: Interaction of the yarns in a UC under the applied symmetric displacements.

The applied displacements cause the development of tensile force, $T_i$, and a contact force, $F_{ci}$, in the yarns. This contact between the two yarns leads to their deformation in the transverse direction denoted by $d_{ci}$. By equilibrium, the resultant contact forces acting on the two yarns should be equal; in other words:

$$F_{c1} = F_{c2} \tag{16}$$

The tensile forces, $T_i$, developed in the yarns are functions of the yarn material and geometrical properties. In this study, the tensile behavior of the Kevlar® 129 yarns is assumed to simply follow a linear elastic model, defined by the equation below:

$$T_i = \frac{E_i A_i}{S_{0i}}\left(S_i - S_{0i}\right) \tag{17}$$

where $E_i$ and $A_i$ are the elastic modulus and cross-sectional area of the fibres in yarn $i$, respectively, and $S_{0i}$ and $S_i$ are the initial and current length of the yarn. The equivalent contact force that develops between the two yarns, $F_c$, can be estimated by enforcing the equilibrium of yarn $i$, as follows:

$$F_{c_i} = 2T_i \sin\alpha_i \tag{18}$$

where $\alpha_i$ is the yarn-end slope (see Figure 3). This slope is calculated using the first derivative of the yarn shape function calculated at the yarn end. Therefore,

$$\sin\alpha_i = \frac{\tan\alpha_i}{\sqrt{1+\tan^2\alpha_i}} = \frac{\pi h_i}{\sqrt{\left(2w_i\right)^2 + \left(\pi h_i\right)^2}} \tag{19}$$

The specific relationship between the transverse contact force acting on the yarns and their compression $d_{ci}$ can be generally expressed as:

$$d_{ci} = Q\left(F_{ci}\right) \tag{20}$$

The relationship considered in this study is assumed to follow the form:

$$d_c = a - \frac{b}{\sqrt[3]{F_c}} \tag{21}$$

where $d_c$ is the total transverse deformation of the fabric, and $a$ and $b$ are constants, determined from transverse compression tests performed on single and multi-ply fabric specimens. The geometric compatibility of the yarn centerlines should also be satisfied considering the original and current shapes of the yarns, transverse deformation of the two yarns and the initial gap, $g$, between them, as shown below:

$$h_1 + h_2 = h_{01} + h_{02} - d_{c1} - d_{c2} - g \tag{22}$$

Equations (16) and (22) are used to determine the two unknowns $h_1$ and $h_2$. Due to the non-linear nature of these two equations, an explicit closed-form solution is not readily obtainable. Therefore, $h_1$ and $h_2$ are calculated using a numerical approach that is capable of solving such multi-variable non-linear system of equations. The Newton-Raphson iterative technique is used to estimate the unknowns $h_1$ and $h_2$ by solving a system of nonlinear equations applied to the objective functions $f_1$ and $f_2$, defined as:

$$f_1 = F_{c1} - F_{c2} \tag{23}$$

$$f_2 = h_1 + h_2 + d_{c1} + d_{c2} + g - h_{01} - h_{02} \tag{24}$$

Figure 4 shows an example of the tensile responses of the warp and weft yarns when the unit-cell is subjected to extension in the warp direction, $d_1$ while the weft yarn is held fixed, i.e. $d_2 = 0$. It can be seen that the interaction of the two yarns causes the tension to build-up in the weft yarn, leading to a biaxial fabric crossover response. The yarns are capable of carrying loads up to their ultimate tensile strength, after which the yarn is considered to have failed and is removed from the calculations. The shell element itself is eroded from the mesh after both the warp and weft yarns reach failure.

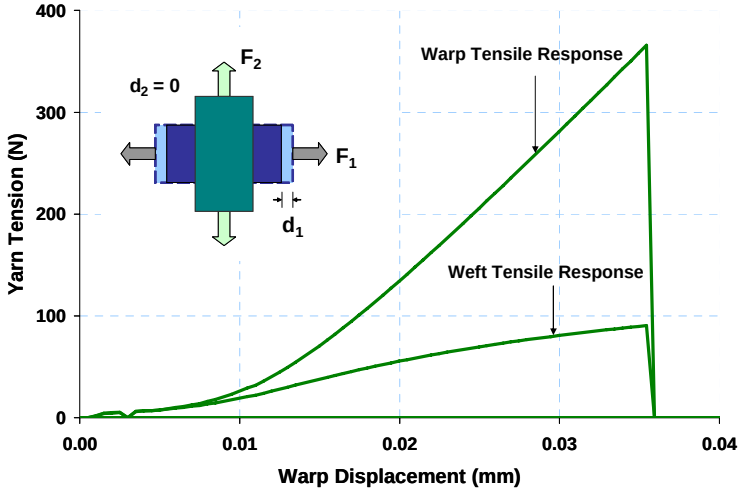


Figure 4: Biaxial response of S-720 unit-cell as a function of warp displacement (weft yarn fixed, $d_2 = 0$), predicted by the 2D shell model. Properties of S-720 fabric panel are listed in Table 1.

Shearing deformation of fabrics is a complicated phenomenon. Experimental investigations show that under pure shearing deformations, most fabrics generally exhibit very low resistance up to a lock-up point. At this point, the resistance quickly builds up as the empty spaces between the yarns are taken up and the yarns start to compact. In order to capture such behavior, a shearing model based on the trellis mechanism is considered [17]. For simplicity, two regimes with distinctly different shear moduli, $G_1$ and $G_2$ ($G_1 << G_2$) are considered, as shown in Figure 5. The shear modulus is assumed to build up between the two user-defined strain values of $\gamma_1$ and $\gamma_2$.

$$G = \begin{cases} G_1 & 0 < |\gamma| \le \gamma_1 \\ G_1 + \dfrac{G_2 - G_1}{\gamma_2 - \gamma_1}(\gamma - \gamma_1) & \gamma_1 < |\gamma| < \gamma_2 \\ G_2 & |\gamma| \ge \gamma_2 \end{cases} \tag{25}$$

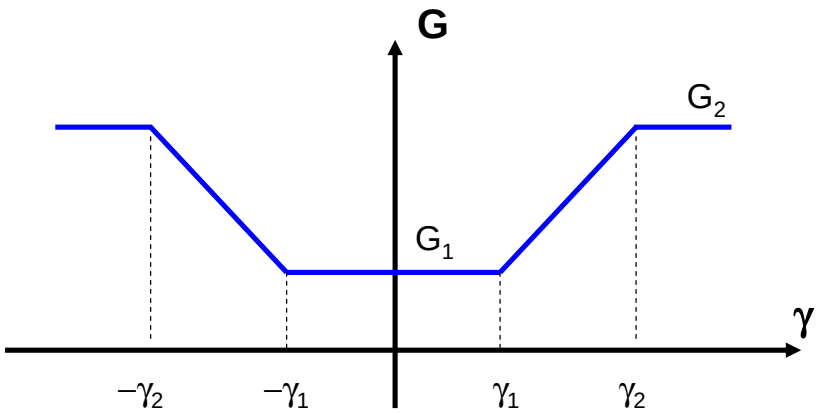


Figure 5: Shear modulus, $G$, as a function of the shear strain, $\gamma$, showing shear hardening (trellising).

The shell element UMAT is now complete with the implementation of the biaxial fabric extensional and shear responses. The next section highlights the results of impact simulations and validation of the model predictions with experimental data.

## Ballistic Impact Simulations

The shell elements coupled with the User Material Model developed above are used to simulate single and multi-ply fabric targets of Kevlar® 129. In doing so, every single fabric cross-over point is replaced with a representative shell element that implicitly comprises a warp and a weft yarn. Ballistic experiments simulated are based on the impact of a blunt-nosed RCC steel projectile of length 42.1 mm and diameter 5.5 mm, with a partially hollowed core so as to achieve a mass of 3 grams, impacting 203 mm by 203 mm square targets of Kevlar® 129 with fixed boundary conditions. The experiments are instrumented with the Enhanced Laser Velocity System (ELVS) [18], which provides a continuous measurement of projectile deceleration during the impact event. Figure 6 shows an example of the projectile velocity-time history predicted by the shell element model compared to the instrumented experimental data for a perforating impact on a 1-ply S-720 target. The mechanical and geometrical properties of S-720 fabric are given in Table I. The model captures the deceleration of the projectile fairly accurately but appears to over-predict the strength of the fabric (and hence its energy absorption capability) as evident

from the under-prediction of the projectile exit velocity. Clearly, this suggests that while the deformation behavior of the fabric is modelled properly, its failure behavior is not. This discrepancy can be due to the fact that not all the failure mechanisms of fibres and yarns are considered in the model, or a result of using the mechanical properties of virgin yarns. The value of yarn failure strain used here, i.e. 3.5%, is nominal and does not reflect the actual value that is probably smaller due to the damage suffered by the yarns during the weaving process.

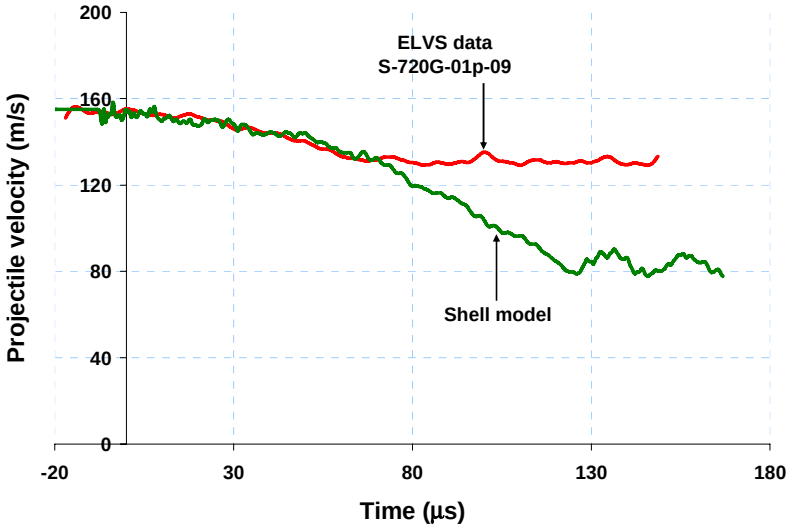


Figure 6: Velocity-time response of an RCC projectile in a perforating impact simulation on a 1-ply S-720 target struck at 155 m/s.

Figure 7 shows the results for a non-perforating impact event involving an S-728 4-ply fabric target (see Table I) impacted at an initial velocity of 91 m/s. Again, it can be seen that the model captures the projectile deceleration during the event and hence the energy absorption of the target fairly well.

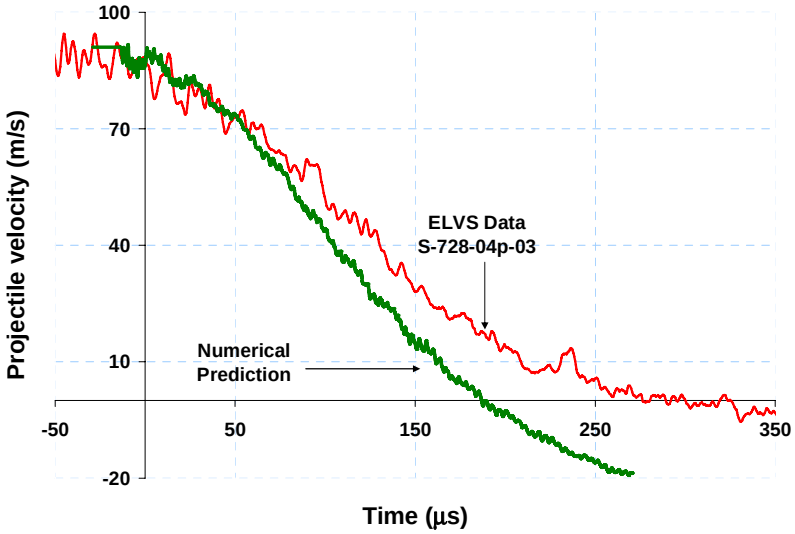


Figure 7: Velocity-time response of an RCC projectile in a non-perforating impact simulation on a 4-ply S-728 target struck at 91 m/s.

Table I: Material and geometrical properties of the fabric panel

| Panel | S-720 | S-728* |
|---|---|---|
| Yarn (denier) | 1420 | 1500 |
| Fibre elastic modulus (GPa) | 96.0 | 96.0 |
| Failure strain (%) | 3.5 | 3.5 |
| Average count (threads per inch) | 20 | 17 |
| Maximum crimp (%) | 2.18 | 1.76 |
| Minimum crimp (%) | 1.39 | 0.94 |
| Areal density ($g/m^2$) | 255.2 | 231.1 |

*S-720 and S-728 are fabric designation used by DuPont, Inc.

## Conclusions

The shell element developed in this study to capture the behavior of plain weave fabrics incorporates the details of weave geometry and yarn properties, such as the their sinusoidal shape, transverse compressive response, warp and weft interaction, etc., in establishing the constitutive relationship for the fabric unit cell. This shell based unit cell, representing a single yarn crossover in a plain weave fabric, is then used to create full models of multi-layer fabric targets subjected to impact by cylindrical projectiles. Successful comparisons have been made between the predictions of the numerical model and the data available from instrumented impact experiments thus demonstrating the ability of the model to capture the complex biaxial behavior of fabric panels. The model developed here can be used as an effective tool to gain insight into the dynamic behavior of fabrics subjected to ballistic threats. This efficient computational model can further be used to carry out parametric studies leading to identification of parameters that most influence the overall energy absorption of fabric armor.

## Acknowledgements

The authors would like to thank the Natural Sciences and Engineering Research Council of Canada (NSERC), DuPont Canada, Defence R&D Canada – Valcartier, and Pacific Safety Products, Inc., for their support of this project. The donation of materials by DuPont is greatly appreciated. We would like to thank Ms. Ingrid Kongshavn and Dr. Elvis Cepuš of the Composites Group at UBC for providing the experimental data used in this work. Thanks are also extended to Dr. Anoush Poursartip for his insight and many fruitful discussions related to the experimental work used for calibration and validation of the model presented here.

### References

1. Roylance, D. and Wang, S. S. 1980. "Penetration mechanics of textile structures," in *Ballistic Materials and Penetration Mechanics*, Elsevier Scientific Publishing Co., pp. 273-292.
2. Shim, V. P. W., C. T. Lim, and K. J. Foo. 2001. "Dynamic mechanical properties of fabric armor," *International Journal of Impact Engineering*, 25: 1-15.
3. Lim, C. T., V. P. W. Shim, and Y. H. Ng. 2003. "Finite element modeling of the ballistic impact of fabric armor," *International Journal of Impact Engineering*, 28: 13-31.
4. Cepus, E., Shahkarami, A., Vaziri, R., and Poursartip, A. 1999. "Effect of boundary conditions on the ballistic response of textile structures," *Proceedings of International Conference on Composite Materials (ICCM 12)*.
5. Shahkarami, A, Vaziri, R., Poursartip, A., and Williams, K. 2002. "A Numerical Investigation of the Effect of Projectile Mass on the Energy Absorption of Fabric Panels Subjected to Ballistic Impact," *Proceedings of 20th International Symposium on Ballistics*, pp. 802-809.
6. Johnson, G. R., Beissel, S. R., and Cunniff, P. M. 1999. "A computational model for fabrics subjected to ballistic impact," *Proceedings of 18th International Symposium on Ballistics*, pp. 962-969.
7. Billon, H. H. and D. J. Robinson. 2001. "Models for the ballistic impact of fabric armor," *International Journal of Impact Engineering*, 25: 411-422.

8. Shockey, D. A., Erlich, D. C., and Simons, J. W. 2000. "Improved barriers to turbine engine fragments," SRI International, Menlo Park, California.
9. Tanov R.R. and M. Brueggert. 2003. "Finite element modeling of non-orthogonal loosely woven fabrics in advanced occupant restraint systems," *Finite Elements in Analysis and Design*, 39: 357-367.
10. Duan, Y., M. Keefe, T. A. Bogetti, and B. A. Cheeseman. 2005. "Modeling friction effects on the ballistic impact behavior of a single-ply high-strength fabric," *International Journal of Impact Engineering*, 31(8): 996-1012.
11. Kawabata, S., M. Niwa, and H. Kawai. 1973. "The finite-deformation theory of plain-weave fabrics Part I: The biaxial-deformation theory," *Journal of the Textile Institute*, 64(2): 21-46.
12. Shahkarami, A. and Vaziri, R. 2005. "An efficient unit-cell based shell element for numerical modelling of fabrics under impact," in *Impact Loading of Lightweight Structures*, M. Alves and N. Jones, eds. WIT Transactions on Engineering Sciences, pp. 451-467.
13. Shahkarami, A, Vaziri, R., Poursartip, A., and Tejani, N. 2005. "An efficient mechanistic approach to modelling the ballistic response of multi-layer fabrics,", pp. 1365-1372.
14. Ivanov, I. and A. Tabiei. 2004. "Loosely woven fabric model with viscoelastic crimped fibres for ballistic impact simulations," *International Journal for Numerical Methods in Engineering*, 61: 1565-1583.
15. King, M. J., P. Jearanaisilawong, and S. Socrate. 2005. "A continuum constitutive model for the mechanical behavior of woven fabrics," *International Journal of Solids and Structures*, 42: 3867-3896.
16. Hallquist, J. O. 2003. *LS-DYNA Keyword User's Manual (Version 970).* Livermore Software Technology Corporation.
17. Tabiei, A. and I. Ivanov. 2002. "Computational micro-mechanical model of flexible woven fabric for finite element impact simulation," *International Journal for Numerical Methods in Engineering*, 53: 1259-1276.
18. Starratt, D., T. Sanders, E. Cepus, A. Poursartip, and R. Vaziri. 2000. "An efficient method for continuous measurement of projectile motion in ballistic impact experiments," *International Journal of Impact Engineering*, 24(2): 155-170.